Applied Physics Letters

RESEARCH ARTICLE | APRIL 09 2024

High temperature stability of entropy-stabilized oxide $(MgCoNiCuZn)_{0.2}O$ in air

Special Collection: Era of Entropy: Synthesis, Structure, Properties, and Applications of High-Entropy Materials

Matthew Webb ; Mike Gerhart; Steven Baksa ; Simon Gelin ; Avery-Ryan Ansbro ; Peter B. Meisenheimer ; Tony Chiang ; Jon-Paul Maria; Ismaila Dabo ; Christina M. Rost ; John T. Heron

Appl. Phys. Lett. 124, 151904 (2024)
https://doi.org/10.1063/5.0199076

AIP Publishing

Applied Physics Letters ARTICLE pubs.aip.org/aip/apl

High temperature stability of entropy-stabilized oxide $(MgCoNiCuZn)_{0.2}O$ in air

Cite as: Appl. Phys. Lett. **124**, 151904 (2024); doi: 10.1063/5.0199076
Submitted: 21 January 2024 · Accepted: 26 March 2024 ·
Published Online: 9 April 2024

Matthew Webb,[1] Mike Gerhart,[2] Steven Baksa,[3] Simon Gelin,[3] Avery-Ryan Ansbro,[1] Peter B. Meisenheimer,[4] Tony Chiang,[1] Jon-Paul Maria,[3] Ismaila Dabo,[3] Christina M. Rost,[2,5] and John T. Heron[1,a)]

AFFILIATIONS

[1]Department of Material Science and Engineering, University of Michigan, Ann Arbor, Michigan 48109, USA
[2]Department of Physics and Astronomy, James Madison University, 901 Carrier Drive, Harrisonburg, Virginia 22807, USA
[3]Department of Materials Science and Engineering, The Pennsylvania State University, University Park, Pennsylvania 16802, USA
[4]Department of Materials Science and Engineering, University of California, Berkeley, California 94720, USA
[5]Department of Materials Science and Engineering, Virginia Polytechnic Institute and State University, Blacksburg, Virginia 24061, USA

Note: This paper is part of the APL Special Collection on Era of Entropy: Synthesis, Structure, Properties, and Applications of High Entropy Materials.
[a)]**Author to whom correspondence should be addressed:** jtheron@umich.edu

ABSTRACT

Entropy-stabilized oxides are single-phase, multicomponent oxides that are stabilized by a large entropy of mixing, ΔS, overcoming a positive enthalpy. Due to the −TΔS term in the Gibbs' free energy, G, it can be hypothesized that entropy-stabilized oxides demonstrate a robust thermal stability. Here, we investigate the high temperature stability (1300–1700 °C) of the prototypical entropy-stabilized rocksalt oxide $(MgCoNiCuZn)_{0.2}O$ in air. We find that at temperatures >1300 °C, the material gradually loses Cu and Zn with increasing temperature. Cu is lost through a selective melting as a Cu-rich liquid phase is formed. Zn is sublimed from the rocksalt phase at approximately similar temperatures to those corresponding to the Cu loss, significantly below both the melting temperature of ZnO and its solubility limit in a rocksalt phase. The elemental loss progressively reduces the entropy of mixing and results in a multiphase solid upon quenching to room temperature. We posit that the high-temperature solubility of Cu and Zn is correlated providing further evidence for entropic stabilization over general solubility arguments.

In recent years, high entropy materials have extended from metal alloys[1–4] to high-entropy and entropy-stabilized oxides (HEOs and ESOs), first with the synthesis of $(MgCoNiCuZn)_{0.2}O$ (herein referred to as (MgCoNiCuZn)O, unless non-equimolar) by Rost *et al.* in 2015.[5] Surrounding these materials is the prospect of high temperature stability due to the large $-T\Delta S$ contribution in Gibbs' free energy, which further stabilizes the structure with increasing T. Due to the relative youth of the field, however, the high temperature stability of HEOs has been investigated in few cases.[6,7] Here, we investigate the high temperature (1300–1700 °C) stability of bulk (MgCoNiCuZn)O, the prototypical ESO.

(MgCoNiCuZn)O is synthesized from the binary rocksalt oxides, MgO, CoO, and NiO, and the binary non-rocksalts, ZnO (wurtzite) and CuO (tenorite),[5] where the Zn^{2+} and Cu^{2+} cations are stabilized into octahedral coordination by the entropy of mixing. This is not without consequences for the crystal, as it has been shown that the local and global structures of (MgCoNiCuZn)O are distorted from an ideal rocksalt, due in part to the Jahn–Teller distortion of the Cu^{2+} ions.[8,9] The structural evolution of (MgCoNiCuZn)O due to this local distortion has been investigated at annealing temperatures up to 800 °C.[10] Despite the significant property changes stemming from these distortions, however, no thorough investigation has been done into the stability of (MgCoNiCuZn)O at higher temperatures. It could be hypothesized that these materials are increasingly stable at elevated temperatures due to the associated increase in entropy or, alternatively, that the stability is dominated by high-temperature solubility

equilibria. In this work, we demonstrate that achieving high temperature stability in entropy stabilized materials is more complex than these hypotheses.

Here, we report the degradation of (MgCoNiCuZn)O at extreme temperatures (>1300 °C) in air, with the loss of Cu and Zn. We hypothesize that the entropy associated with the melting of CuO clusters encourages the loss of Cu from the structure, and that local distortions and defects around Cu^{2+} ions will result in greater diffusion rates for ions at elevated temperatures. This enables phase segregation and net removal of these ions from the (MgCoNiCuZn)O pellet, increasing the ionicity of the rocksalt grains and causing a change in morphology. Furthermore, we posit that the loss of Cu and the associated decrease in entropy leave Zn as the high energy (enthalpy) constituent in a nominal three-component ~ $(MgCoNi)_{0.33}O$ rocksalt alloy, resulting in a correlated effect between the loss of Cu and the loss of Zn.

In this work, our samples consist of ~5 × 5 × 2.5 mm^3 fragments of single-phase, polycrystalline (MgCoNiCuZn)O that was derived from a single sintered pellet. The pellet was prepared by mixing and grinding the constituent powders [MgO, CoO, NiO, CuO, and ZnO (all Alfa Aesar, 99.99%)], then pressing at 70 000 psi, and sintering at 1100 °C for 18 h before air quenching to room temperature. This procedure is performed twice to ensure homogeneity. A homogeneous and nominally equimolar composition of the pellet was confirmed using scanning electron microscopy energy dispersive spectroscopy (SEM EDS). All composition analysis was conducted using a Thermo Fisher Nova 200 Nanolab SEM/FIB. Samples were mounted to an Al stub using conductive C tape. The SEM EDS was conducted using a 20 kV accelerating voltage, 0.6 nA probe current, and ~500× magnification. Images were taken using an Everhart–Thornley detector. EDS was performed at a minimum of three different locations on each pellet within a particle. EDS quantification and mapping were done using the $K\alpha_1$ transitions for each element.

After confirming the composition, the pellet was fragmented, to undergo separate high temperature annealing treatments and subsequent characterization. Individual polycrystalline (MgCoNiCuZn)O samples were annealed at 1300, 1400, 1500, 1600, and 1700 °C in air using a SentroTech ST-1700 °C bottom loading furnace. All samples were placed on a bed of (MgCoNiCuZn)O powder contained within an alumina crucible and introduced to the furnace at the target temperature and held at this temperature for 2 h before air quenching.

SEM EDS analysis reveals inhomogeneity in the annealed samples. Images in Fig. 1 were produced using the Cu concentration maps to color SEM images of the same region. In samples annealed between 1300 and 1600 °C, we observe isolated, non-grain regions of high Cu concentration between rocksalt particles. At high temperatures, we anticipate that regions of tenorite CuO segregate within the rocksalt particles, melting to form a Cu rich liquid phase that is solidified into an amorphous phase upon quenching. At 1300 °C, a significant amount of Cu remains in the rocksalt particles commensurate with smaller segregated Cu deposits. At the highest temperatures, the lower viscosity of the Cu-rich liquid allows most of it to drain from the pellet before quenching occurs, leaving fused rocksalt particles. Volume fraction analysis was performed using ImageJ Software,[11] and results are shown in the supplementary material, Fig. S1. Note that the Zn EDS signal is homogenous even in the dilute limit annealed at the highest temperatures (shown in the supplementary material, Fig. S2), indicating Zn is sublimating from the rocksalt particles, rather than segregating. It has been shown computationally that the local strain around Cu^{2+} and Zn^{2+} ions reduces the formation energy of cation vacancies;[12] we theorize that this expected higher vacancy concentration around these ions results in greater mobilities at these high temperatures, allowing clustering and net diffusion of these ions out of the rocksalt structure.

In the regime of annealing temperatures from 1300 to 1500 °C, particle size also increases significantly from the pristine sample. At low temperature, the samples appear as smooth, round particles with a significant density of pores, filled by Cu-rich material. The sample annealed at 1600 °C is in an intermediate state, where the particles are still round with some porosity, filled in by liquid Cu during the anneal, with striated facets beginning to emerge. Above this regime, after

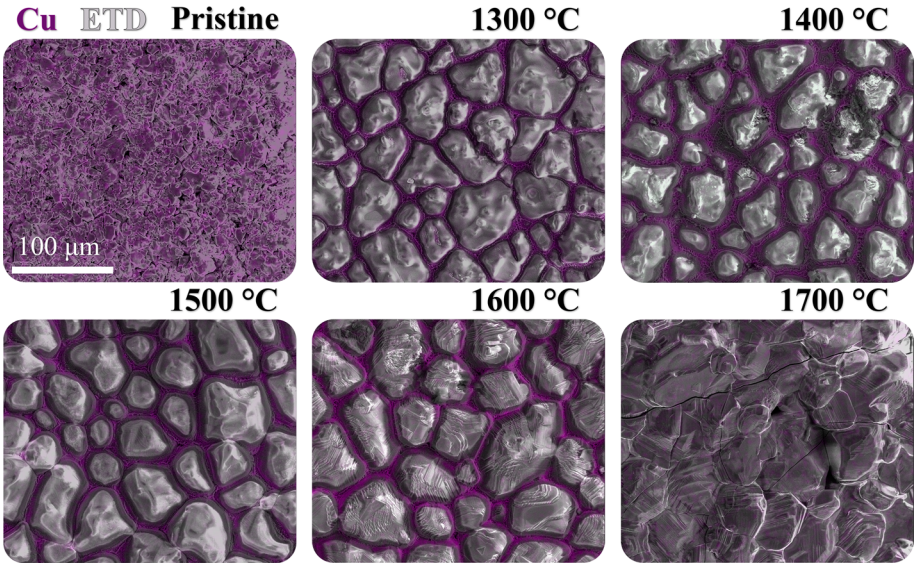

FIG. 1. Composition and morphology of (MgCoNiCuZn)O sintered pellets following high temperature annealing. SEM EDS of pellet following annealing at up to 1700 °C showing inhomogeneous distribution of Cu following annealing. Regions of high Cu concentration are observed between rocksalt particles after annealing. The rocksalt particles are homogeneous in Mg, Co, Ni, and Zn, with a decreasing Zn concentration with increasing temperature due to sublimation. There is still a non-zero Cu concentration in the rocksalt particles; however, it is not easy to see in the EDS maps due to the much larger segregated Cu concentration. Images were taken using an Everhart–Thornley detector (ETD) and colored using the Cu concentration maps collected using EDS. Raw SEM images of all annealed pellets can be found in the supplementary material.

annealing at 1700 °C, the pores have disappeared, and the particles have fused completely, striated with clear facets. This emergence of faceting is consistent with an increased ionicity of the alloy as Zn and Cu concentrations are reduced. Large intragranular cracks are observed across the pellet, likely due to the high thermal strains that are expected during quenching. Raw SEM images of all annealed pellets and SEM EDS maps can be found in the supplementary material (Figs. S2 and S3).

The phases of the annealed samples were determined by x-ray diffraction (XRD) at room temperature post-quench. 2θ–ω scans were performed with a Rigaku Smartlab diffractometer, using a 1.54 Å Cu Kα source, a Ni filter, Bragg–Brentano geometry, a 10 mm slit at 4°/min, and with a 0.1° step size. The 2θ–ω scans reveal diffraction peaks consistent with a rocksalt structure and a lattice parameter of 4.239 ± 0.001 Å (determined by Rietveld refinement using International Center for Diffraction Data's Powder Diffraction File PDF-5[13] 00-073-0933) in agreement with prior reports of bulk (MgCoNiCuZn)O.[5,9,14,15] XRD spectra of a pristine sample and samples after annealing are shown in Fig. 2. All the peaks identified in the XRD belong to the rocksalt system; no wurtzite, tenorite or other secondary phase peaks are observed. This further indicates that the residual Cu-rich phase is amorphous and present no evidence of wurtzite (ZnO) or tenorite (CuO) phases in the annealed samples. An unusual trend is observed in the peak intensity ratios of the annealed samples, and that the I_{200}/I_{220} ratio decreases from 1300 to 1500 °C before increasing again when the annealing temperature is increased further. This is seen to inversely correlate with the Cu-rich fraction (supplementary material, Fig. S1), and this correlation is shown in the supplementary material, Fig. S4, along with further discussion.

We investigated the evolution of the composition (by SEM EDS) with annealing temperature to understand the chemistry of the emergent phases. The sample composition and ideal configurational entropy for equimolar 3-, 4-, and 5-component oxides (and the temperature-entropy product) are shown in Fig. 3, plotted against annealing temperature. Elemental analysis of samples annealed at temperatures above 1400 °C shows a significant deviation of composition, with Zn and Cu being lost from the pellet. At temperatures 1500 °C and higher, a significantly increased Mg concentration is observed. From cross-sectional EDS of the sample annealed at 1600 °C, it has been confirmed that this increase Mg concentration is primarily at the surface (supplementary material, Fig. S5). We hypothesize that this is a result of the strain introduced by quenching the sample. Using the experimentally determined composition, Fig. 3(b) plots the expected lattice parameter using Vegard's law[16] and the Shannon ionic radii[17] for these compositions along with the lattice parameters as determined

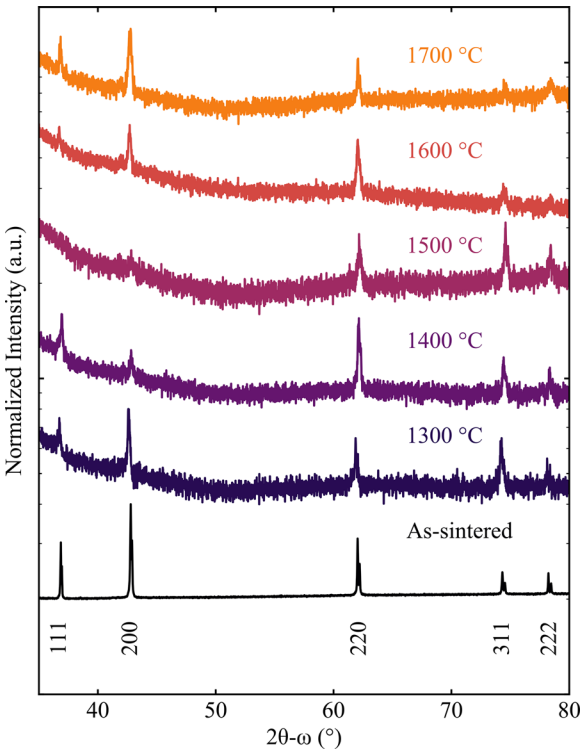

FIG. 2. X-ray diffraction patterns following high temperature anneal of (MgCoNiCuZn)O. X-ray diffraction data for an as-sintered pellet (1100 °C for 18 h) of polycrystalline (MgCoNiCuZn)O and the same (MgCoNiCuZn)O pellet after annealing for 2 h at the given temperature and subsequent air quench. The peak intensity ratios for the as-sintered sample are typical of a rocksalt structure; however, following annealing, the peaks broaden, and the intensity ratios shift to a more intense 220 peak. This could be an indication of change in local structure. No tenorite or wurtzite secondary phases are observed. Datasets are offset vertically for clarity.

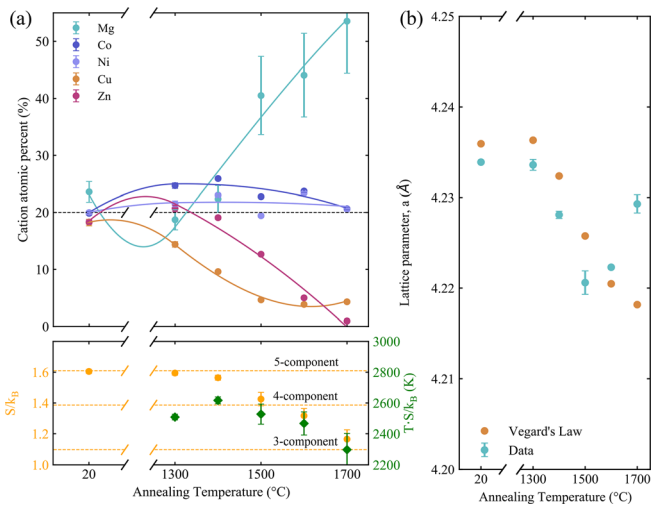

FIG. 3. Selective loss of Cu and Zn at high temperature in (MgCoNiCuZn)O. (a) SEM EDS data showing the cation atomic percent of a rocksalt particle surface, following a 2-h dwell at the given temperature. The 20 °C sample is as-sintered and has not undergone an annealing treatment. Errors are the error in the fit according to the SEM software. Lines have been added to help guide the eye along the changes in each elemental composition and sum to 100%. Additionally, the calculated configurational entropy (S) of each composition is shown in the bottom panel, along with the TS product. The dotted lines represent the expected S/k values for ideal five-, four-, and three-component systems, respectively. We observe that significant losses in Cu and Zn occur, and correspondingly, this results in a drop in entropy. (b) The experimental lattice parameters and errors as determined using Rietveld refinement for the Kα1 peaks in Fig. 2, along with the Vegard's law estimate using the compositions from (a). The Vegard's law[16] calculation was done using experimental values for MgO, CoO, and NiO, and using the octahedrally coordinated ionic radii[17] for Cu^{2+} and Zn^{2+}, to estimate the lattice parameter of rocksalt CuO and ZnO. While individual points have poor correlation, the overall trend between the change in Vegard's law and the measured lattice parameter is similar.

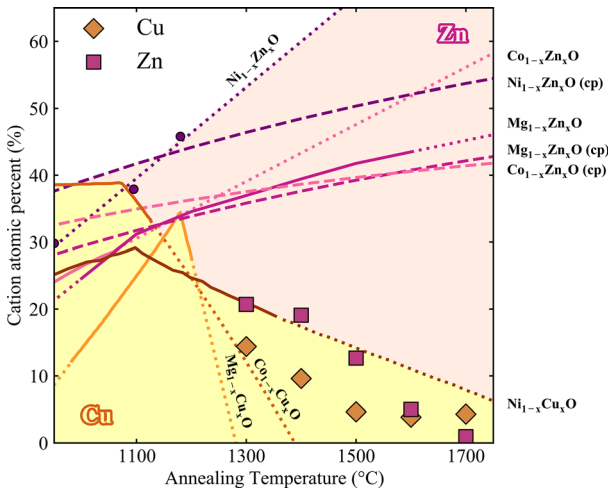

FIG. 4. Comparison of observed Cu and Zn composition to maximum solubility at the solidus. The shaded area indicates the maximum range of miscibility based off only the binary rocksalt-CuO and rocksalt-ZnO systems. The copper concentration in (MgCoNiCuZn)O is observed to correspond roughly with the solubility of Cu in the rocksalt-Cu oxide binary systems in the 1300–1700 °C range. We note the observed Zn composition in (MgCoNiCuZn)O is much lower than the maximum solubilities in the associated binary oxide constituents, and that the Cu and Zn concentrations are correlated. Dotted lines indicate linearly extrapolated data. Dashed lines (cp) indicate calculated data (details in the supplementary material, Fig. S6). Ni-Cu solubility data from the solidus in the NiO-CuO phase diagram.[20] The same is true, respectively, for the MgO-ZnO,[25] CoO-CuO,[21] MgO-CuO,[22] CoO-ZnO,[23] and NiO-ZnO systems. The NiO-ZnO data are shown as individual points as it is obtained from the NiO-ZnO axis of a ternary Fe_2O_3-NiO-ZnO[24] phase diagram as no NiO-ZnO data could be found.

using Rietveld refinement from Fig. 2 data. The general agreement between Vegard's law and the experimental lattice parameter indicates that the quantified composition is correctly identified as belonging to the rocksalt phase, thus a reasonable basis to estimate ideal configurational entropy form.

Using the ideal configurational entropy[18] for a system with compositions $\{x_i\}$

$$S_{\text{conf}} = -k_B \sum_i x_i \ln(x_i).$$

The compositional changes correspond to an entropy change from ~1.60 to ~1.16 k_B. For an ideal five-component system, S_{conf} is 1.61 k_B, in a four-component system, it is 1.39 k_B, and in a three-component system, it is 1.10 k_B (see Fig. 3). The drop in the ideal configurational entropy of the pellet also leads to a decrease in $-T\Delta S$. This change in entropy to below that of a four-component oxide supports a hypothesis that Zn sublimes from the rocksalt phase due to the entropy no longer being sufficient to counteract an unfavorable enthalpy.

The entropy-stabilization hypothesis has been challenged by suggesting that general solubility of the species dictates the formation of (MgCoNiCuZn)O.[19] Under this hypothesis, the loss of Cu and Zn from the compound would be due to the solubility limit decreasing with increasing temperature. Considering the case of $Cu_xNi_{1-x}O$, the Cu maximum solubility[20] at the solidus closely matches the Cu concentration we observe in Fig. 2(a) over the relevant temperature range. This comparison is shown in Fig. 4. Generally, the Cu and Zn binary compounds do not correlate strongly with our data.[21–25] Aside from $Cu_xNi_{1-x}O$ which shows high solubility, the other Cu binaries exhibit much lower solubilities for Cu than observed, while all the Zn binaries suggest far higher solubility. It is important to note that the high temperature MgZnO solubility in air has been reported,[25] and this correlates well with the computed data as well as trends in the other ZnO binaries. Based on this discrepancy, a general solubility argument is insufficient to explain the formation and stability of (MgCoNiCuZn)O.

We posit that the correlation between the Zn and Cu composition is an entropy driven effect. Cu has the least favorable enthalpy toward the rocksalt structure, and prior density functional theory calculations indicate that the Cu cation is associated with the largest point defect densities in the crystal.[12] From an intuitive enthalpic and kinetic

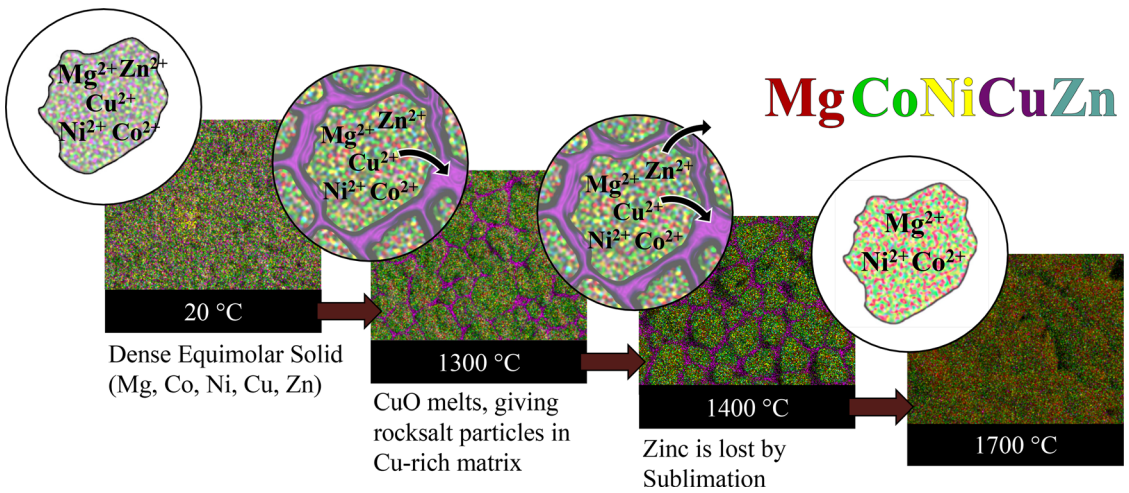

FIG. 5. Summary of the degradation of entropy-stabilized oxide (MgCoNiCuZn)O. At 20 °C, in the pristine state, a roughly equimolar dense solid made of small rocksalt particles is observed. Upon annealing at 1300 °C, Cu is segregated into a liquid phase that then solidifies into an amorphous phase along the grain boundaries upon cooling. When further annealed to 1400 °C, Zn sublimates from the rocksalt phase and is lost. Upon annealing to 1700 °C, once again a dense rocksalt solid is observed; however, it is now primarily comprised of Mg, Co, and Ni, as Cu and Zn concentrations have significantly reduced.

perspective, Cu can be expected to segregate first from the structure. If CuO segregates at ≳1300 °C, it would be expected to melt, decreasing total entropy of the alloy. While the addition of ZnO to a single-cation rocksalt, such as MgO, generally has high solubility limits (Fig. 4), we expect that this limit is lower in the four-component system due to the diminishing return of gained entropy with more species, i.e., the entropy change from a one to two cation system is much greater than that from a three to four component system. It then follows that when the Cu and associated entropy is lost from the structure, the solubility for Zn also decreases, causing the correlation in composition that we observe, as the unfavorable enthalpy is no longer compensated. The main findings of this work, the loss of Cu by melting above 1300 °C and the loss of Zn by sublimation above 1400 °C, are summarized schematically in Fig. 5.

In this work, we show that (MgCoNiCuZn)O, the prototypical entropy-stabilized oxide, phase separates at high temperatures in air. This has been observed through a change in structure, composition, and particle morphology, following annealing treatments at temperatures up to 1700 °C. The material loses a significant fraction of both Cu and Zn at temperatures >1300 °C in correlation. We anticipate that local cation vacancies around the Cu and Zn result in larger mobilities for these ions, allowing them to cluster and segregate from the (MgCoNiCuZn)O through selective melting and sublimation. Furthermore, the correlative loss of Zn indicates that the formation of the (MgCoNiCuZn)O is not due to general solubility.

See the supplementary material for details on scanning electron microscopy images, compositional mapping for all samples, and analysis of XRD intensities and computed ZnO-MO phase diagrams.

This work was supported by the National Science Foundation through awards NSF MRSEC DMR-2011839 and NSF CAREER under Grant No. DMR-1847847. The authors acknowledge the financial support of the University of Michigan College of Engineering, NSF Grant No. DMR-0420785, and NSF Grant No. DMR-0320740, and technical support from the Michigan Center for Materials Characterization. The phase diagram calculations were performed using the Rockfish cluster at the Advanced Research Computing at Hopkins (ARCH) core facility, through allocation PHY220113 from the Advanced Cyberinfrastructure Coordination Ecosystem: Services & Support (ACCESS) program, which is supported by NSF Grant Nos. 2138259, 2138286, 2138307, 2137603, and 2138296.

AUTHOR DECLARATIONS

Conflict of Interest

The authors have no conflicts to disclose.

Author Contributions

Matthew Webb: Conceptualization (equal); Investigation (equal); Methodology (equal); Visualization (equal); Writing – original draft (equal); Writing – review & editing (equal). **Mike Gerhart:** Investigation (supporting); Methodology (supporting). **Steven Baksa:** Investigation (supporting); Methodology (supporting). **Simon Gelin:** Investigation (supporting); Methodology (supporting). **Avery-Ryan Ansbro:** Investigation (supporting); Methodology (supporting). **Peter B. Meisenheimer:** Conceptualization (equal); Investigation (supporting); Writing – review & editing (supporting). **Tony Chiang:** Investigation (supporting). **Jon-Paul Maria:** Conceptualization (supporting); Writing – review & editing (supporting). **Ismaila Dabo:** Investigation (supporting); Methodology (supporting). **Christina M. Rost:** Conceptualization (supporting); Investigation (supporting); Methodology (supporting); Writing – review & editing (supporting). **John T. Heron:** Conceptualization (equal); Investigation (equal); Methodology (equal); Writing – original draft (equal); Writing – review & editing (equal).

DATA AVAILABILITY

The data that support the findings of this study are available from the corresponding author upon reasonable request.

REFERENCES

[1]B. Cantor, "Multicomponent and high entropy alloys," Entropy **16**(9), 4749 (2014).
[2]M.-H. Tsai and J.-W. Yeh, "High-entropy alloys: A critical review," Mater. Res. Lett. **2**(3), 107–123 (2014).
[3]B. E. MacDonald, Z. Fu, B. Zheng, W. Chen, Y. Lin, F. Chen, L. Zhang, J. Ivanisenko, Y. Zhou, H. Hahn, and E. J. Lavernia, "Recent progress in high entropy alloy research," JOM **69**(10), 2024–2031 (2017).
[4]J. Chen, X. Zhou, W. Wang, B. Liu, Y. Lv, W. Yang, D. Xu, and Y. Liu, "A review on fundamental of high entropy alloys with promising high–temperature properties," J. Alloys Compd. **760**, 15–30 (2018).
[5]C. M. Rost, E. Sachet, T. Borman, A. Moballegh, E. C. Dickey, D. Hou, J. L. Jones, S. Curtarolo, and J.-P. Maria, "Entropy-stabilized oxides," Nat. Commun. **6**(1), 8485 (2015).
[6]H. Chen, J. Fu, P. Zhang, H. Peng, C. W. Abney, K. Jie, X. Liu, M. Chi, and S. Dai, "Entropy-stabilized metal oxide solid solutions as CO oxidation catalysts with high-temperature stability," J. Mater. Chem. A **6**(24), 11129–11133 (2018).
[7]G. N. Kotsonis, C. M. Rost, D. T. Harris, and J.-P. Maria, "Epitaxial entropy-stabilized oxides: Growth of chemically diverse phases via kinetic bombardment," MRS Commun. **8**(3), 1371–1377 (2018).
[8]P. B. Meisenheimer, L. D. Williams, S. H. Sung, J. Gim, P. Shafer, G. N. Kotsonis, J.-P. Maria, M. Trassin, R. Hovden, E. Kioupakis, and J. T. Heron, "Magnetic frustration control through tunable stereochemically driven disorder in entropy-stabilized oxides," Phys. Rev. Mater. **3**(10), 104420 (2019).
[9]C. M. Rost, Z. Rak, D. W. Brenner, and J.-P. Maria, "Local structure of the $Mg_xNi_xCo_xCu_xZn_xO$(x = 0.2) entropy-stabilized oxide: An EXAFS study," J. Am. Ceram. Soc. **100**(6), 2732–2738 (2017).
[10]D. Berardan, A. K. Meena, S. Franger, C. Herrero, and N. Dragoe, "Controlled Jahn–Teller distortion in (MgCoNiCuZn)O-based high entropy oxides," J. Alloys Compd. **704**, 693–700 (2017).
[11]C. A. Schneider, W. S. Rasband, and K. W. Eliceiri, "NIH image to ImageJ: 25 years of image analysis," Nat. Methods **9**(7), 671–675 (2012).
[12]S. Chae, L. Williams, J. Lee, J. T. Heron, and E. Kioupakis, "Effects of local compositional and structural disorder on vacancy formation in entropy-stabilized oxides from first-principles," npj Comput. Mater. **8**(1), 95 (2022).
[13]The International Centre for Diffraction Data-ICDD, see https://www.icdd.com/ for "crystallographic data" (2024).
[14]P. B. Meisenheimer, T. J. Kratofil, and J. T. Heron, "Giant enhancement of exchange coupling in entropy-stabilized oxide heterostructures," Sci. Rep. **7**(1), 13344 (2017).
[15]C. M. Rost, D. L. Schmuckler, C. Bumgardner, M. S. Bin Hoque, D. R. Diercks, J. T. Gaskins, J.-P. Maria, G. L. Brennecka, X. Li, and P. E. Hopkins, "On the thermal and mechanical properties of $Mg_{0.2}Co_{0.2}Ni_{0.2}Cu_{0.2}Zn_{0.2}O$ across the high-entropy to entropy-stabilized transition," APL Mater. **10**(12), 121108 (2022).
[16]L. Vegard, "Die konstitution der mischkristalle und die raumfüllung der atome," Z. Phys. **5**(1), 17–26 (1921).

[17]R. D. Shannon, "Revised effective ionic radii and systematic studies of interatomic distances in halides and chalcogenides," Acta Cryst. A **32**(5), 751–767 (1976).
[18]F. Tian, "A review of solid-solution models of high-entropy alloys based on *ab initio* calculations," Front. Mater. **4**, 36 (2017).
[19]M. Fracchia, M. Coduri, M. Manzoli, P. Ghigna, and U. A. Tamburini, "Is configurational entropy the main stabilizing term in rock-salt $Mg_{0.2}Co_{0.2}Ni_{0.2}Cu_{0.2}Zn_{0.2}O$ high entropy oxide?," Nat. Commun. **13**(1), 2977 (2022).
[20]H. Eric and M. Timuçin, "Equilibrium relations in the system nickel oxide-copper oxide," Metall. Trans. B **10**(4), 561–563 (1979).
[21]L. A. Zabdyr and O. B. Fabrichnaya, "Phase equilibria in the cobalt oxide-copper oxide system," J. Phase Equilib. **23**(2), 149 (2002).
[22]A. Gadalla and J. White, "Equilibrium relationships in the system CuO–Cu_2O–MgO," Trans. J. Br. Ceram. Soc. **63**, 119–134 (1964).
[23]C. Ma and A. Navrotsky, "Thermodynamics of the CoO–ZnO system at bulk and nanoscale," Chem. Mater. **24**(12), 2311–2315 (2012).
[24]A. B. Juan, C. Clausell-Terol, J. C. J. Fonfría, and M. M. Fuster, "The influence of green microstructure and sintering parameters on precipitation process during copper-nickel-zinc ferrites sintering," Bol. Soc. Esp. Ceram. Vidrio **53**, 69–75 (2014).
[25]L. Xia, Z. Liu, and P. Taskinen, "Solubility study of the halite and wurtzite solid solutions in the MgO–ZnO system within temperature range from 1000 to 1600 °C," J. Alloys Compd. **687**, 827–832 (2016).